Hydrology Research

Hydrology Research Vol 54 No 4, 435 doi: 10.2166/nh.2023.061

Decomposition of contribution to runoff changes and spatial differences of major tributaries in the middle reaches of the Yellow River based on the Budyko framework

Yanyu Dai [a,b,c], Fan Lu[a,*], Benqing Ruan[a], Xinyi Song[d], Yu Du[a] and Yiran Xu[a]

[a] State Key Laboratory of Simulation and Regulation of Water Cycle in River Basin, China Institute of Water Resources and Hydropower Research, Beijing 100038, China
[b] College of Hydrology and Water Resources, Hohai University, Nanjing 210098, China
[c] Department of Geography, National University of Singapore, Arts Link, Kent Ridge 117570, Singapore
[d] School of Hydraulic and Environmental Engineering, Changsha University of Science & Technology, Changsha 410114, China
*Corresponding author. E-mail: lufan@iwhr.com

YD, 0000-0002-4598-7887

ABSTRACT

Quantitative differentiation of climate and human activities on runoff is important for water resources management and future water resources trend prediction. In recent years, runoff in the middle reaches of the Yellow River (MRYR) has decreased dramatically. Many studies have analyzed the causes of runoff reduction, but there is still a lack of understanding of the spatial differences in runoff contributions and their causes. Therefore, this study quantitatively distinguishes the contributions of climate and human activities to runoff changes in nine sub-basins of the MRYR based on the Budyko framework and analyses the differences in the contributions of different basins and their causes. The results show that the runoff in the nine sub-basins decreases significantly and the precipitation increases from northwest to southeast. The contribution of human activities to runoff is greater than that of climate change, especially in the Huangfuchuan (HF) River and Kuye (KY) River basins, where the contribution of human activities to runoff exceeds 90%. The greater impact of human activities in HF River and KY River is due to the significantly higher water use growth rate and normalized vegetation index trends than in other areas.

Key words: Budyko, climate change, human activities, runoff, Yellow River

HIGHLIGHTS

- Spatial differences in the causes of runoff variation in nine small watersheds in the middle reaches of the Yellow River were analyzed.
- The influence of NDVI and human water extraction cannot be ignored.

GRAPHICAL ABSTRACT

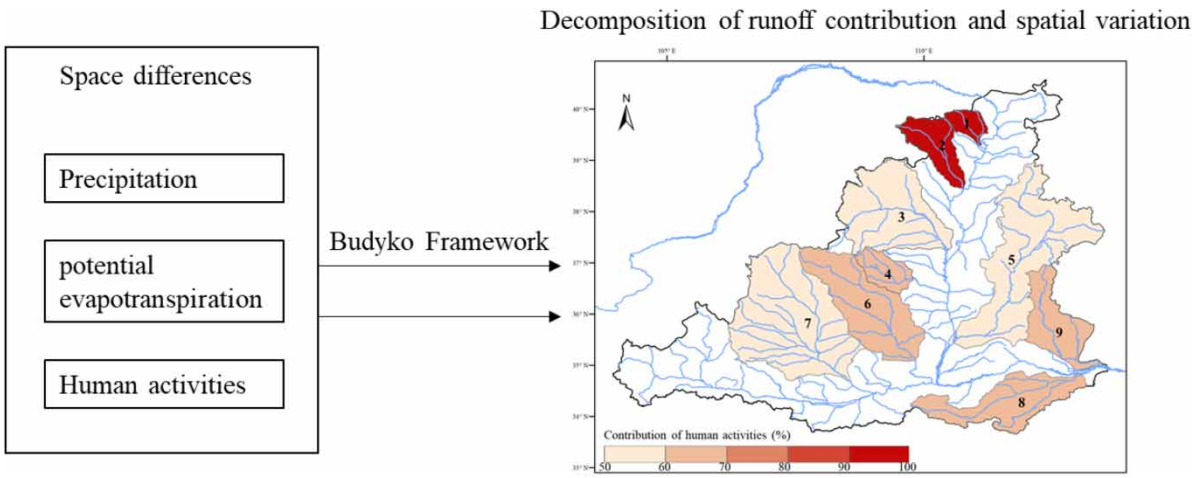

1. INTRODUCTION

Climate change directly affects the abundance and depletion of runoff, while human activities change the underlying surface conditions through land-use/land-cover changes and the construction of water conservancy facilities, thereby affecting the process of yielding and runoff. In recent years, the evolution and vulnerability of water resources under changing environments have been a research focus in academia. Climate change and human activities are two important factors in changing environments, and their impact on the hydrological cycle has received extensive attention (Barnett *et al.* 2005; Piao *et al.* 2010), with a range of methods deployed including statistical methods (Hou *et al.* 2018; Luan *et al.* 2021), meteorological–hydrological methods (Wang *et al.* 2018a, 2018b), hydrological models (Zhai & Tao 2017), and elastic coefficient methods based on the Budyko framework (Tang & Wang 2021). The statistical method requires less data, and the calculation process is simple but lacks a physical basis. The meteorological–hydrological method mainly includes the climatic elasticity method and the hydrological sensitivity method, which are mainly used for analysis on long-time scales and do not reflect changes in the flow process (Wang *et al.* 2018a, 2018b). The hydrological model has a clear physical mechanism and can undertake multi-time scale analysis and calculation but requires high quality and quantity of input data and has large uncertainties (Leavesley 1994). The elastic coefficient method based on the Budyko framework has been widely used because of its reliable physical basis and simple calculation process (Wang *et al.* 2020).

Since the 1950s, the availability of water and sand in the Yellow River basin has decreased sharply due to the influence of climate and human activities, with the most obvious decline in the middle reaches (Zhao *et al.* 2013; Li *et al.* 2014). In recent years, many studies have evaluated the contribution of climate and human activities to runoff by considering the middle reaches as a whole or selecting a particular tributary (Li *et al.* 2018, 2019; Liu *et al.* 2021; Yu *et al.* 2021; Ni *et al.* 2022). The Budyko framework is an important method for decomposing the contribution of runoff changes and has been widely used in studying the contribution of vegetation (Wang *et al.* 2021; Ji *et al.* 2022), soil and water conservation measures (Liang *et al.* 2015; Yu *et al.* 2021), constructions of reservoirs/dams (Tian *et al.* 2019), and climate change (Zheng *et al.* 2021; Ni *et al.* 2022) to runoff in the middle reaches of the Yellow River (MRYR) and its sub-basins.. Liu *et al.* (2021) found that human activities contributed 62% (1987–2003) and 59% (2004–2016) to the reduction of runoff in the MRYR compared to the base period (1965–1986) by comparing the measured runoff with the 'natural runoff'. But in the Wuding (WD) River Basin, Yu *et al.* (2021) found that precipitation was the main factor in runoff reduction in the 1970s–1990s compared to the base period of 1957–1971, and the influence of vegetation measures gradually increased and became dominant after 2000. Therefore, it is necessary to use consistent methods and data from the same period to clarify the causes of runoff changes in each tributary of the MRYR. It also provides the essential basis for subsequent site-specific water resource management.

In this study, we first analyzed the trends of hydrometeorological elements by Mann–Kendall (M-K) trend analysis, then divided the study period into two periods: the base period and the abrupt change period by M–K abrupt change analysis, and calculated the coefficients of substratum in the two periods by Budyko's water-heat balance equation. Finally, the effects of precipitation, potential evapotranspiration, and underlying surface parameter on runoff were calculated by using the elasticity coefficient method to quantify the contribution of climate change and human activities to runoff changes in nine sub-basins in the MRYR. Comparing and analyzing hydrometeorological elements and changes in the sub-basins can provide a theoretical basis for future water resources management and protection in the middle reaches.

2. MATERIALS AND METHODS

2.1. Study area and data

The MRYR is located between Toudaoguai and Huayuankou hydrological stations (Figure 1). The watershed covers 344,000 km^2, accounting for 45.7% of the area of the Yellow River basin. The influence of terrain and other factors, the spatial distribution of precipitation in the basin is uneven, and it generally decreases from southeast to northwest. Most of the tributaries in the MRYR are located in the Loess Plateau, where heavy rains are concentrated. The soil in the midstream area is loose and surface gullies are crisscrossed, making the midstream area the main sand-producing area of the Yellow River basin. From upstream to downstream, the main hydrological stations of the MRYR are mainly Toudaoguai, Longmen, Sanmenxia, and Huayuankou.

The terrain of the MRYR is high in the northwest and low in the southeast with the terrain dominated by plateaus. The main landforms in the study area include loess hilly and gully area, residual plateau area, northwest aeolian sand area, loess terrace area, alluvial plain, and rocky mountainous area. Vegetation transitioned from the warm temperate deciduous broad-leaved

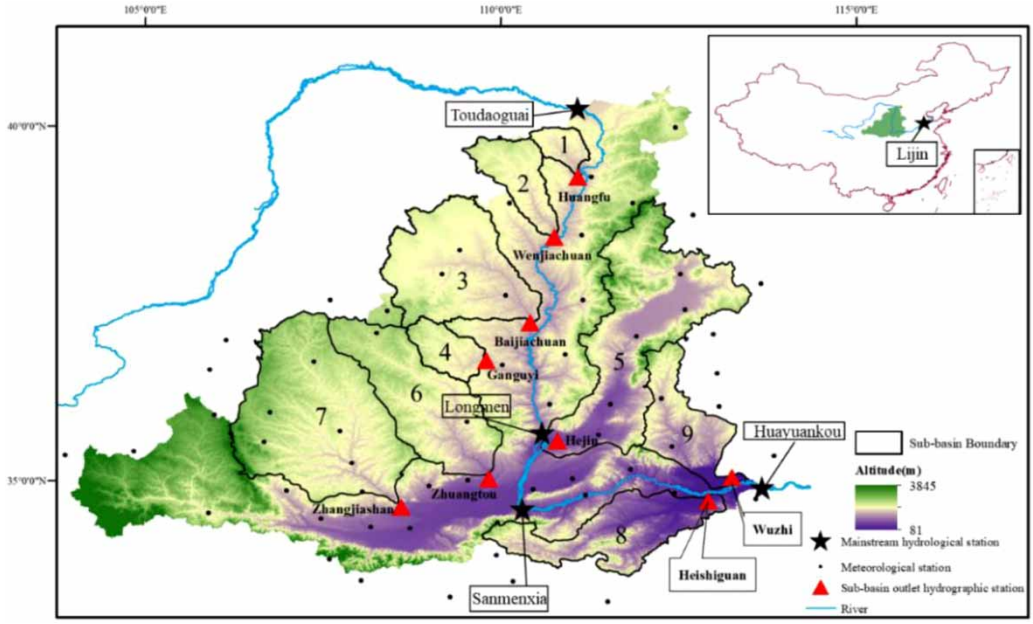

Figure 1 | Middle reaches of the Yellow River.

forest belt to the temperate grassland belt from south to north. Except for a few rocky mountainous areas, most areas of the study area are covered by loess with deep soil layers. The main soils are loess soil, cinnamon soil, and black loam soil.

There are eight main tributaries in the MRYR, including Huangfuchuan (HF) River, Kuye (KY) River, Wuding (WD) River, Yan River (YR), Wei River, and Yiluo (YL) River on the right bank, and Fen River (FR) and Qin River (QR) on the left bank. Among them, the Weihe River is the largest tributary of the Yellow River, with a drainage area of 134,800 km^2. The larger tributaries of the Weihe River are mostly concentrated on the north bank. Among them, the major tributaries larger than 10,000 km^2 are the Hulu River, the Jing River (JR), and the Beiluo (BL) River. The FR is the second-largest tributary of the Yellow River and the largest river in Shanxi Province. Many important industrial cities are concentrated in the basins of the FR. The QR and the YL River are one of the main sources of floods in the Yellow River. Because of their proximity to the lower reaches of the Yellow River, the occurrence of floods poses a great threat to the lower reaches. The typical middle reaches selected in this study are HF River, KY River, WD River, YR, FR, JR, BL River, QR, and YL River (Figure 1 and Table 1), which basically cover the entire MRYR.

This study uses the meteorological data of 54 meteorological stations in and around the MRYR from 1960 to 2020 (Figure 1), including average, maximum/minimum temperature, precipitation, average wind speed, sunshine hours, relative humidity, etc. Data are obtained from the China Meteorological Scientific Data Sharing Service Network (https://www.

Table 1 | Study area

ID	Basin	Area (10,000 km^2)	Outlet hydrologic station
1	HF	0.32	Huangfu
2	KY	0.87	Wengjiachuan
3	WD	2.97	Baijiachuan
4	YR	0.59	Ganguyi
5	FR	3.97	Hejin
6	BL	2.69	Zhuangtou
7	JR	4.54	Zhangjiashan
8	YL	1.89	Heishiguan
9	QR	1.35	Wuzhi

nmic.cn/). The potential evapotranspiration (E_0) is calculated using the Penman–Monteith formula recommended by the Food and Agriculture Organization of the United Nations (FAO). The mean areal precipitation and E_0 in each river basin are calculated using the Thiessen polygon method calculation. The annual runoff data of each hydrological station were obtained from the Hydrological Bureau of the Yellow River Water Conservancy Commission. Human water withdrawal data are from the Yellow River Water Resources Bulletin for 1990–2020. Digital Elevation Model (DEM) data come from Geodata Spatial Cloud (http://www.gscloud.cn/). The land-use data come from the global land cover (GLC) data set (Global Land Surface Satellite-GLC (GLASS-GLC)) published by Liu *et al.* (2020) with a spatial resolution of 5 km × 5 km, including annual data from 1982 to 2015. The normalized vegetation index (NDVI) data come from the National Earth System Science Data Center, National Science & Technology Infrastructure of China (http://www.geodata.cn), with a spatial resolution of 5 km.

2.2. Methods

2.2.1. Budyko hydrothermal coupling balance equation

Former Soviet climatologist Budyko found that long-term evapotranspiration from the land surface can be determined by moisture and energy input. In long-time series analysis, precipitation (P) can be used as water input, and potential evapotranspiration (E_0) can be used as energy input. Under different climate conditions, land surface evapotranspiration (E) satisfies the following boundary conditions: (1) In extremely dry areas, all precipitation is converted into land surface evapotranspiration, (2) In extremely humid areas, all energy used for the potential evapotranspiration is converted into latent heat (Budyko 1974; Fu 1981), there are:

$$\begin{cases} \dfrac{E_0}{P} \to \infty,\ \dfrac{E}{P} \to 1(\text{Extremely dry}) \\ \dfrac{E_0}{P} \to 0,\ \dfrac{E}{P} \to 1(\text{Extremely humid}) \end{cases} \tag{1}$$

Satisfying the above boundary conditions, the general expression of the hydrothermal coupling balance equation considering water balance and energy balance is:

$$\frac{E}{P} = f\left(\frac{E_0}{P}\right) \tag{2}$$

Usually, $\varepsilon = \dfrac{E_0}{P}$, ε is the drought index, and $f(\cdot)$ is assumed to be a universal function that satisfies all watersheds. For a closed watershed, its long-term water balance equation can be expressed as:

$$P = Q + E + \Delta S \tag{3}$$

where Q is the runoff, and ΔS is the water storage variable in the basin, which can usually be ignored in the long-sequence analysis.

$$Q = P - E = P - Pf(\varepsilon) \tag{4}$$

According to the universal function $f(\cdot)$, the land surface evapotranspiration can be expressed as:

$$E = \{P \cdot E_0 \cdot [1 - \exp(-\varepsilon)] \cdot \tan h(\varepsilon)\}^{0.5} \tag{5}$$

Considering the differences in regional climate and geography, scholars have successively proposed various empirical formulas based on Budyko's theory. Previous studies have shown that the hydrothermal coupling balance equation considering the characteristic parameters of the underlying surface can simulate the annual runoff in various catchments in China (Xing *et al.* 2018) (Table 2). In this study, the Fu Baopu formula (Table 2) was used for analysis and calculation (Fu 1981).

Table 2 | Hydrothermal coupled equilibrium equation based on Budyko hypothesis

Method	Formula
Choudhury-Yang	$f(\varepsilon\|n) = \frac{E_0}{(P^n + E_0^n)^{1/n}}$
Fu	$f(\varepsilon\|n) = 1 + \varepsilon - (1 + \varepsilon^n)^{\frac{1}{n}}$
Zhang	$f(\varepsilon\|n) = \frac{[1 + n\varepsilon]}{\left[1 + n\varepsilon + \frac{1}{\varepsilon}\right]}$
Wang-Tang	$f(\varepsilon\|n) = \frac{\{1 + \varepsilon - [(1+\varepsilon)^2 - 4n(2-n)\varepsilon]^{0.5}\}}{[2n(2-n)]}$

Note: The underlying surface parameter (n) reflects the watershed characteristics and is a function of vegetation type, soil properties, and topographical characteristics.

2.2.2. Sensitivity analysis

Assuming that P, E_0, and n are independent variables in Fu's equation (Table 2), combined with the water balance equation, the total differential form of the runoff in the basin is:

$$dQ = \frac{\partial Q}{\partial P}dP + \frac{\partial Q}{\partial ET_0}dET_0 + \frac{\partial Q}{\partial n}dn \tag{6}$$

The sensitivity of runoff (Q) to various influencing factors can be expressed by the elastic coefficient ϕ, $\phi_P = dQ/Q/dP/P$ is the elastic coefficient of precipitation, $\phi_{E_0} = dQ/Q/dE_0/E_0$ is the elastic coefficient of potential evapotranspiration, and $\phi_n = dQ/Q/dn/n$ is the elastic coefficient of the underlying surface.

$$\frac{dQ}{Q} = \phi_P\frac{dP}{P} + \phi_{E_0}\frac{dE_0}{E_0} + \phi_n\frac{dn}{n} \tag{7}$$

$$\mu = \frac{E_0}{P} \tag{8}$$

The elastic coefficient expressions are

$$\phi_P = \frac{(1+\mu^n)^{1/n+1} - \mu^{n+1}}{(1+\mu^n)[(1+\mu^n)^{1/n} - \mu]} \tag{9}$$

$$\phi_{E_0} = \frac{1}{(1+\mu^n)[1 - (1+\mu^n)^{1/n}]} \tag{10}$$

$$\phi_n = \frac{\ln(1+\mu^n) + \mu^n \ln(1+\mu^{-n})}{\mu(1+\mu^n)[1 - (1+\mu^n)^{1/n}]} \tag{11}$$

The positive and negative values of the elastic coefficient represent the positive and negative correlation between the influence factor and the runoff, and the absolute value represents the degree of influence of the influence factor on the runoff.

2.2.3. Runoff contribution breakdown

Under the combined action of climate change and human activities, the changes in watershed runoff can be expressed as:

$$\Delta R = \Delta R_c + \Delta R_n \tag{12}$$

ΔR is the total change in runoff; ΔR_c is the change in runoff caused by climate change; ΔR_n is the change in runoff caused by human activities.

$$\Delta R_c = \Delta R_P + \Delta R_{E_0} \tag{13}$$

ΔR_P is the change in runoff due to changes in precipitation; ΔR_{E_0} is the change in runoff due to changes in potential evapotranspiration.

$$\Delta R_P = \phi_P \frac{R}{P}\Delta P, \quad \Delta R_{E_0} = \phi_{E_0} \frac{R}{E_0}\Delta E_0, \quad \Delta R_n = \phi_n \frac{R}{n}\Delta n \tag{14}$$

ΔP, ΔE_0, and Δn are the changes of precipitation, potential evapotranspiration, and underlying surface coefficients in the change period relative to the base period, respectively.

3. RESULTS

3.1. Characteristics of hydrometeorological changes

The variation trends of precipitation, potential evapotranspiration, and runoff in the MRYR and nine sub-basins were analyzed by linear propensity estimation and the M–K trend test (Mann 1945). The results are shown in Figure 2 and Table 3. Precipitation in the five northern sub-basins (HF, KY, WD, YR, FR) is significantly less than that in the four southern sub-basins (BL, JR, YL, QR). The maximum annual precipitation (YL) is 1.6 times greater than the minimum annual precipitation (KY). Precipitation increases in the western sub-basins and decreases in the east. However, the potential evapotranspiration in the northern sub-basins is significantly larger than that in the southern sub-basins, indicating that the northern sub-basin is drier. Except for a significant decrease in precipitation in the QR ($p < 0.01$), all other basins showed a non-significant trend in precipitation. Potential evapotranspiration decreased significantly in HF ($p < 0.05$), YL, and QR ($p < 0.01$) and increased significantly in WD, FR, and BL ($p < 0.01$), while the trend was not significant in the other basins. Runoff in the nine sub-basins showed a significant decreasing trend ($p < 0.01$).

Figure 3 and Table 4 show the abrupt change point of runoff in the MRYR and nine sub-basins from 1960 to 2020. Among them, abrupt change points in FR and QR are significantly earlier (before 1975) than the rest. Abrupt change points can be detected around 1998 (HF, YR, and BL), and 1989 (KY and JR). Runoff in WD and YL experienced significant variation after the 1980s (1981 and 1985, respectively). For each sub-basin, the historical records before the abrupt change point were used as the base period (Period I), and the rest was used as the runoff in the change period (Period II) for follow-up research.

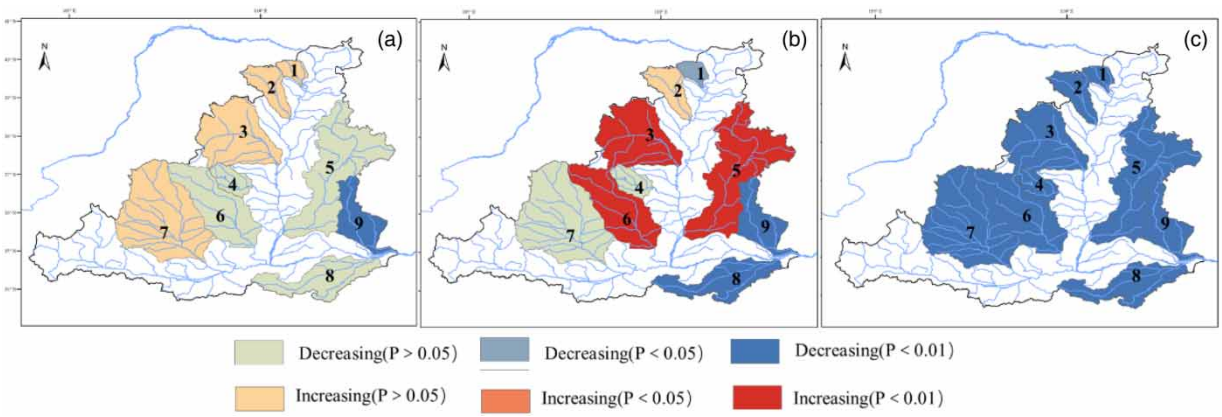

Figure 2 | Spatial distribution of the results of M–K trend analysis of hydrometeorological variables for 1960–2020 ((a) precipitation; (b) potential evapotranspiration; (c) runoff).

Table 3 | Hydrometeorological data change trend in the study area from 1960 to 2020

	Basin	Mean annual (mm)	Slope (mm/year)
Precipitation	HF	411.6	−0.05
	KY	411.0	0.30
	WD	417.2	0.41
	YR	463.7	−0.69
	FR	465.4	−0.65
	BL	542.0	−0.67
	JR	540.7	0.28
	YL	657.7	−0.75
	QR	579.4	−1.46***
	MRYR	512.6	−0.15
Potential evapotranspiration	HF	973.5	−0.86**
	KY	1,060.5	0.36*
	WD	1,081.1	1.08***
	YR	1,002.6	0.01
	FR	1,022.1	0.59***
	BL	932.6	0.68***
	JR	917.7	0.17
	YL	1,068.7	−1.00***
	QR	961.2	−0.87***
	MRYR	994.8	0.28
Runoff	HF	32.3	−1.00***
	KY	56.4	−1.25***
	WD	35.5	−0.42***
	YR	33.0	−0.28***
	FR	21.7	−0.51***
	BL	30.5	−0.33***
	JR	35.6	−0.46***
	YL	120.6	−1.80***
	QR	49.0	−1.26***
	MRYR	40.4	−0.76***

Note: *, **, and *** represent significance levels of 0.1, 0.05, and 0.01, respectively.

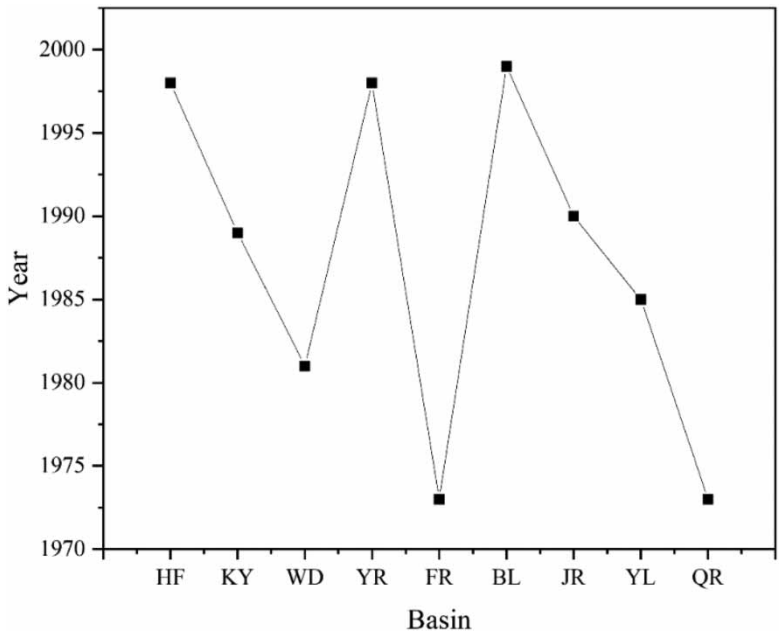

Figure 3 | Abrupt change point of runoff in the middle Yellow River from 1960 to 2020.

Table 4 | Abrupt change point of runoff in the study area from 1960 to 2020

Basin	Abrupt change point
HF	1998
KY	1989
WD	1981
YR	1998
FR	1973
BL	1999
JR	1990
YL	1985
QR	1973

3.2. Decomposition of contributions of meteorological and underlying surface changes to runoff changes

3.2.1. Sensitivity analysis of runoff to climate change and human activities

Table 5 shows the multi-year average precipitation (P), potential evapotranspiration (E_0), runoff depth (Q), underlying surface parameter (n) (calculated using Fu's equation), and the elasticity coefficients of the three influencing factors (ϕ_p, ϕ_{E_0}, ϕ_n), calculated using Equations (9)–(11) for the study area during Period I and Period II. Figure 4 shows the relative rate of change in Period II compared to Period I (i.e., Figure 4 = (variable in Period II – variable in Period I) × 100/variable in Period I).

Compared with Period I, the precipitation in WD and BL slightly increased in Period II. However, the precipitation in other sub-basins showed decreasing trends, especially in QR, FR, and YL (Figure 4(a)). Meanwhile, the potential evapotranspiration in these three sub-basins decreased in Period II (with a larger relative decrease in the QR), while the other basins increased (Figure 4(b)).

Except for precipitation (P, Figure 4(a)) and potential evapotranspiration (E_0, Figure 4(b)), other variables changed consistently in all sub-basins. Runoff (Figure 4(d)) and runoff coefficients (Figure 4(e)) decreased in nine sub-basins, while the ratio of

Table 5 | Hydrometeorological characteristics and elastic coefficients of the study area during Period I and Period II

Basin	Period	P (mm)	E_0 (mm)	Q (mm)	n	Q/P	E_0/P	ϕ_p	ϕ_{E_0}	ϕ_n
HF	I	413.4	968.7	45.2	2.49	0.11	2.34	2.41	−1.41	−3.07
	II	408.5	982.1	9.6	3.75	0.02	2.40	3.70	−2.70	−4.25
KY	I	409.3	1,051.7	77.7	1.99	0.19	2.57	1.92	−0.92	−2.85
	II	412.6	1,069.1	35.8	2.56	0.09	2.59	2.49	−1.49	−3.39
WD	I	425.6	1,066.1	45.0	2.44	0.11	2.51	2.37	−1.37	−3.20
	II	412.5	1,089.6	30.2	2.66	0.07	2.64	2.60	−1.60	−3.54
YR	I	467.7	996.1	37.2	2.90	0.08	2.13	2.80	−1.80	−3.13
	II	456.7	1,014.1	25.7	3.14	0.06	2.22	3.06	−2.06	−3.45
FR	I	500.1	1,031.0	41.6	2.91	0.08	2.06	2.80	−1.80	−3.05
	II	455.1	1,019.4	15.8	3.57	0.03	2.24	3.50	−2.50	−3.83
BL	I	538.6	921.9	34.4	3.63	0.06	1.71	3.46	−2.46	−2.88
	II	548.6	953.0	23.2	4.10	0.04	1.74	3.96	−2.96	−3.20
JR	I	548.8	907.4	43.5	3.46	0.08	1.65	3.27	−2.27	−2.67
	II	532.2	928.4	27.4	3.84	0.05	1.74	3.68	−2.68	−3.06
YL	I	690.5	1,085.5	160.3	2.24	0.23	1.57	2.07	−1.07	−2.01
	II	633.4	1,056.3	91.0	2.71	0.14	1.67	2.53	−1.53	−2.33
QR	I	635.6	998.3	93.8	2.79	0.15	1.57	2.58	−1.58	−2.21
	II	562.6	950.1	35.7	3.68	0.06	1.69	3.51	−2.51	−2.86

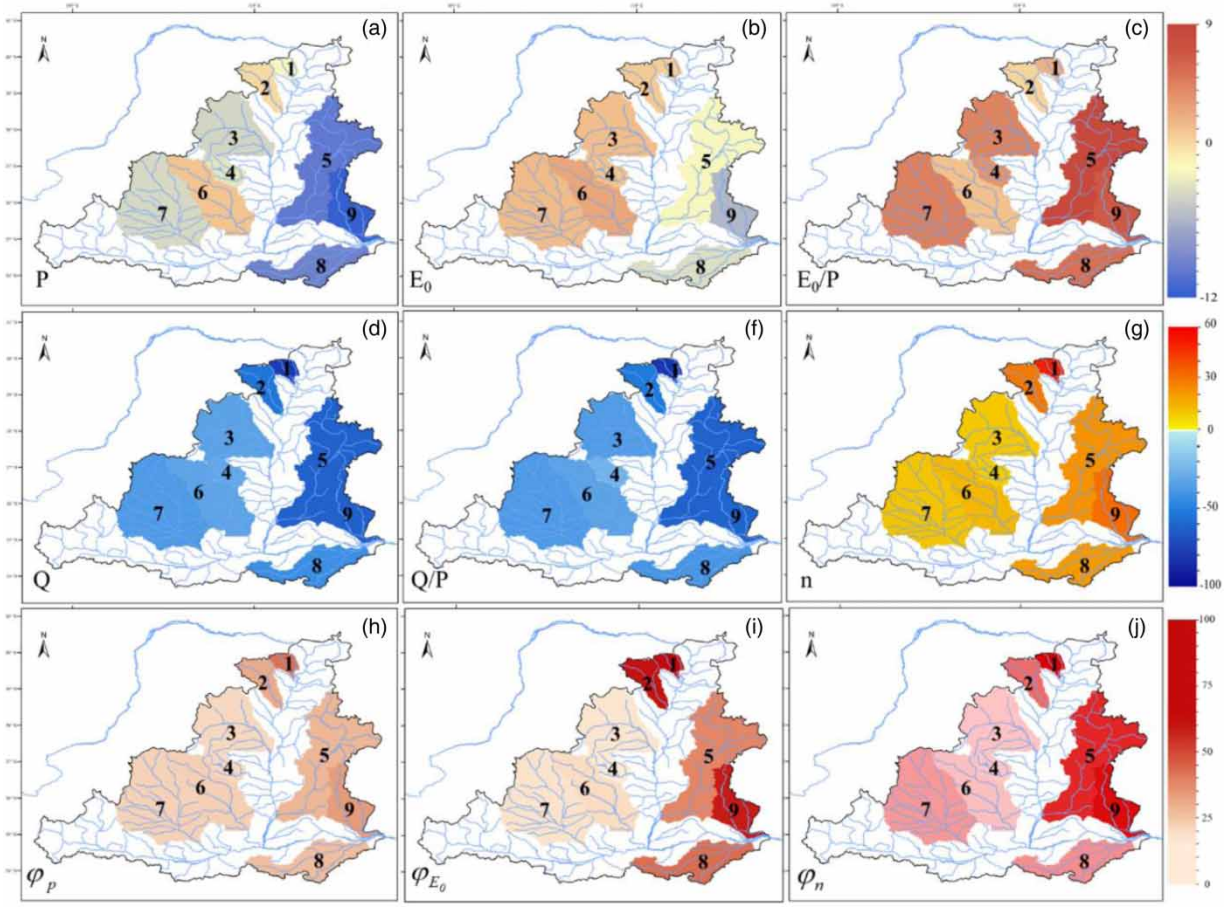

Figure 4 | Rate of change for the period before the abrupt change point (Period I) and after (Period II) (%).

potential evapotranspiration to precipitation (E_0/P, Figure 4(c)) and underlying surface parameter (n) (Figure 4(f)) increased. The runoff was more sensitive to changes in precipitation, potential evapotranspiration, and underlying surface parameter (n) (Figure 4(g)–4(i)). Among the basins with large changes are mainly HF, FR, and QR.

3.2.2. Runoff change contribution

In this section, we will quantitatively distinguish the reasons for the change of runoff before and after the abrupt points in nine sub-basins. Table 6 shows the total runoff change (ΔR) in Period II relative to Period I, the meteorological factors (ΔR_C) – precipitation (ΔR_P) and potential Evapotranspiration (ΔR_{E_0}), and the amount of runoff change caused by human activities ($\triangle R_n$), and its proportion in the total runoff change. The calculation results show that the runoff of the nine sub-basins during Period II is reduced compared with Period I, and both climate change and human activities in the study area have led to the reduction of runoff. Human activities are the main reasons for the reduction of watershed runoff, but the contribution rate varies. The largest contribution of human activities ($\triangle R_n/\triangle R$) to runoff can be detected in KY and HF (>90%). The contribution rate of human activities in other watersheds is more than 55% (Table 6, Figure 5). Previous studies have also confirmed that human activities are the main reason for the reduction of runoff in the MRYR (Shi *et al.* 2012; Kong *et al.* 2016).

4. DISCUSSION

4.1. Causes of spatial variation in runoff variability attribution

From 1960 to 2020, the runoff of the Yellow River basin decreases at a rate of 5.63×10^8 m^3/year, of which MRYR account for 46.3% (Figure 6). The change of runoff in MRYR significantly affects the runoff of the whole Yellow River basin. There are

Table 6 | Contribution of climate change and human activities in the study area

Basin	$\triangle R$ (mm)	$\triangle R_P$ (mm)	$\triangle R_{E_0}$ (mm)	$\triangle R_C$ (mm)	$\triangle R_C/\triangle R$ (%)	$\triangle R_n$ (mm)	$\triangle R_n/\triangle R$ (%)
HF	−35.6	−1.5	−1.3	−2.8	7.6	−32.9	92.4
KY	−41.9	8.6	−10.4	−1.8	4.2	−40.1	95.8
WD	−14.8	−4.3	−1.9	−6.2	42.0	−8.6	58.0
YR	−11.6	−2.7	−1.4	−4.1	35.3	−7.5	64.7
FR	−25.8	−12.2	1.0	−11.2	43.4	−14.6	56.6
BL	−11.2	10.1	−13.6	−3.5	31.4	−7.7	68.6
JR	−16.0	−4.7	−2.5	−7.2	44.9	−8.8	55.1
YL	−69.3	−28.9	5.5	−23.4	33.8	−45.9	66.2
QR	−58.1	−31.3	8.9	−22.4	38.6	−35.7	61.4

Note: The change of runoff is negative, indicating that the runoff in Period II is less than in Period I. The runoff change is positive, indicating that the runoff in Period II is increased compared with Period I.

over 30 major tributaries (catchment area greater than 1,000 km^2) in MRYR, and these tributaries account for 44% of the flow in the Yellow River basin (Zhao *et al.* 2014). The contribution of the nine sub-basins involved in this study to the attenuation of the Yellow River runoff was proportional to the size of the sub-basins. The largest contribution was made by YL with 6.04% (Figure 7). In addition, there are significant differences in climate and underlying surface conditions between the northern and southern parts of MRYR. Therefore, it is important to explore the regional differences in hydrological processes in response to future climate change and the intensification of human activities in the Yellow River basin.

From 1960 to 2020, the MRYR showed a non-significant decreasing trend in precipitation and potential evapotranspiration, but a significant decrease in runoff (Table 3), indicating the importance of human activities on runoff generation in the region.

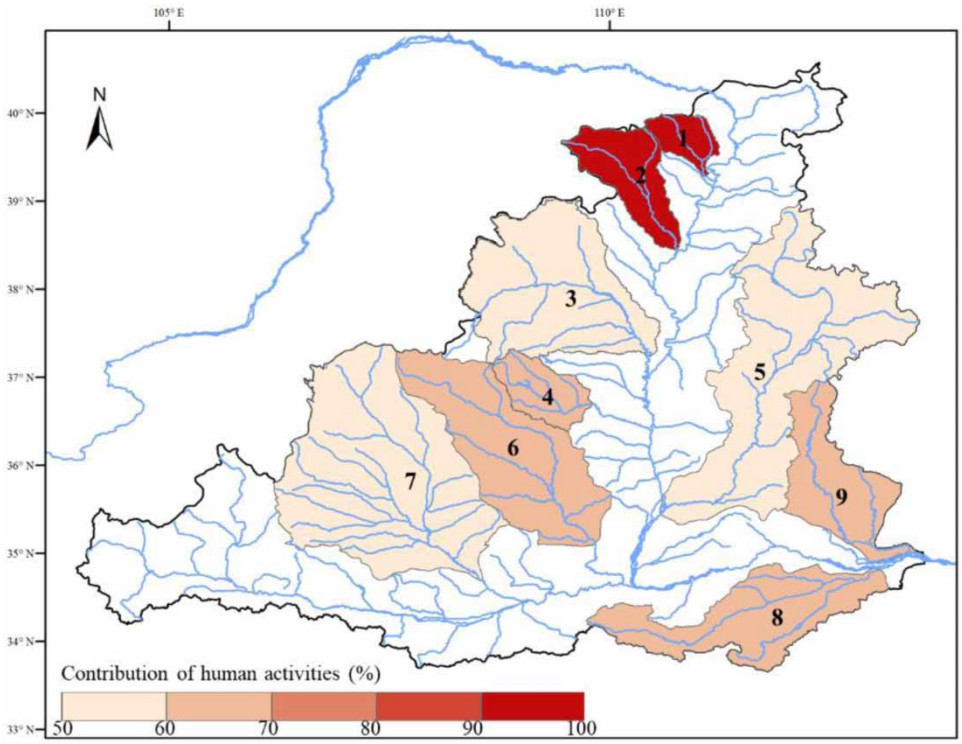

Figure 5 | Spatial distribution of the contribution of human activities to runoff.

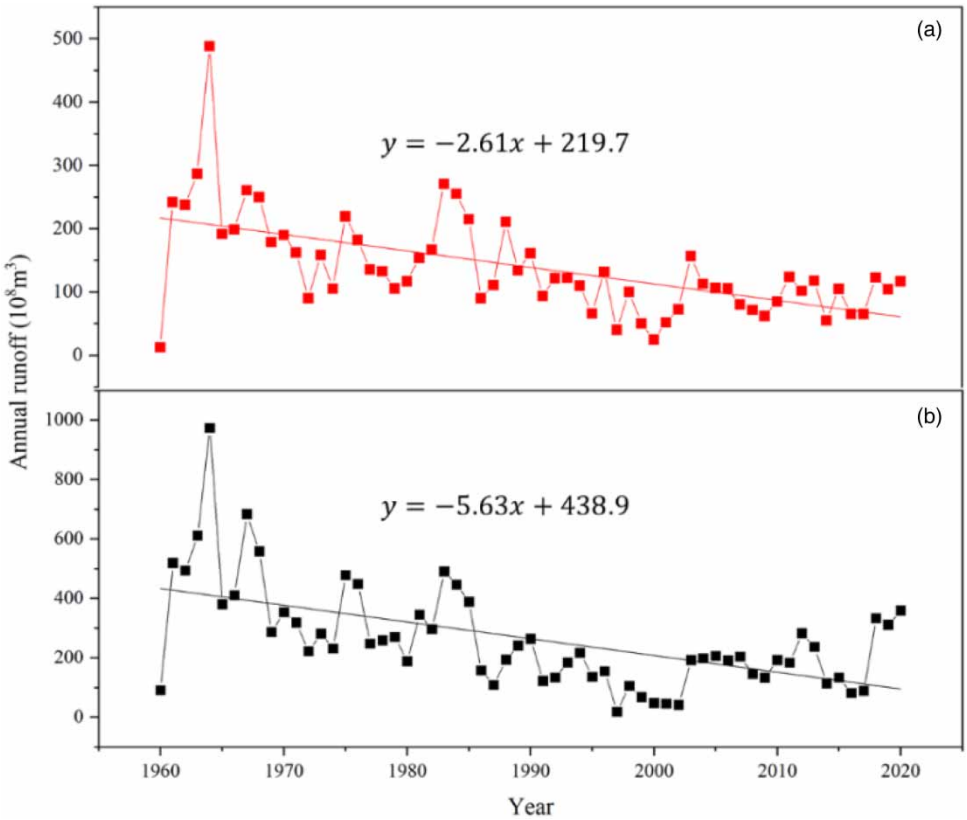

Figure 6 | Variations in runoff in MRYR (a) and the whole basin (b) of the Yellow River from 1960 to 2020.

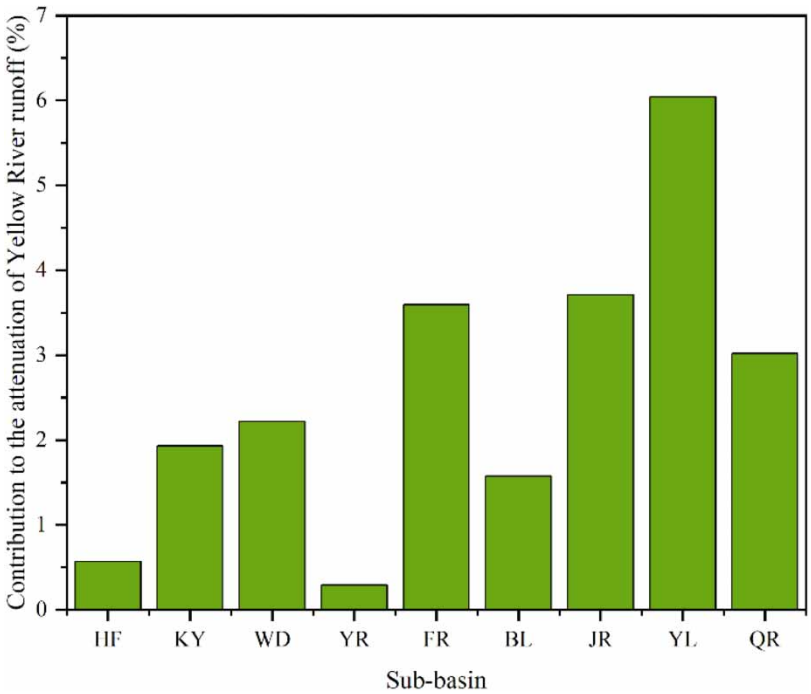

Figure 7 | Contribution of sub-basins to the attenuation of runoff in the Yellow River basin.

This is also responsible for the spatial variation in human and climate change contributions across the nine sub-basins in this study.

Since the 1960s, a series of soil and water conservation measures have been implemented in the MRYR. The area of soil and water conservation has increased from 8.47×10^3 km^2 in 1969 to 107.9×10^3 km^2 in 2015 in the section from Toudaoguai to Tongguan (Zhao *et al.* 2021). Currently, about one-third of the region has adopted different soil and water conservation measures, with afforestation accounting for more than 60% and terracing for about 25% of the area (Liu *et al.* 2021). The reduction of runoff due to vegetation restoration has been proven globally, especially for runoff in arid regions (Liang *et al.* 2015; Zhang *et al.* 2018). There are two main reasons for this: first, the increase in vegetation cover leads to a decrease in surface albedo, leading to higher temperatures, resulting in increased evapotranspiration (Li *et al.* 2016). In addition, afforestation and grass planting increase the potential of precipitation interception, improving the soil structure and infiltration (Miao *et al.* 2010; Xu 2011). A study by Sun *et al.* (2006) concluded that revegetation in the Loess Plateau region might lead to a 50% reduction in runoff. Using the improved Budyko formula, Ji *et al.* (2022) calculated that NDVI changes contributed 33.37% to the reduction of runoff in MRYR. The multi-year mean NDVI of the nine sub-basins from 1982 to 2020 gradually increased from north to south (Table 7; Figure 8(a)). Each of the nine sub-basins showed a noticeable increase in NDVI between 1982 and 2020 ($p < 0.01$). Figure 8(b) shows the growth rate of the multi-year average NDVI for 2000–2020 compared to 1982–1999. It can be seen that the NDVI growth rates in the four northern sub-basins (HF, KY, WD, YR) are significantly larger than those in the other basins.

Table 7 | Multi-year average and growth rate of NDVI in nine sub-basins

Basin	Annual average	Growth rate (%)
HF	0.21	21.6
KY	0.21	25.2
WD	0.21	27.3
YR	0.28	36.8
FR	0.34	13.7
BL	0.37	20.1
JR	0.31	19.1
YL	0.42	14.9
QR	0.39	15.8

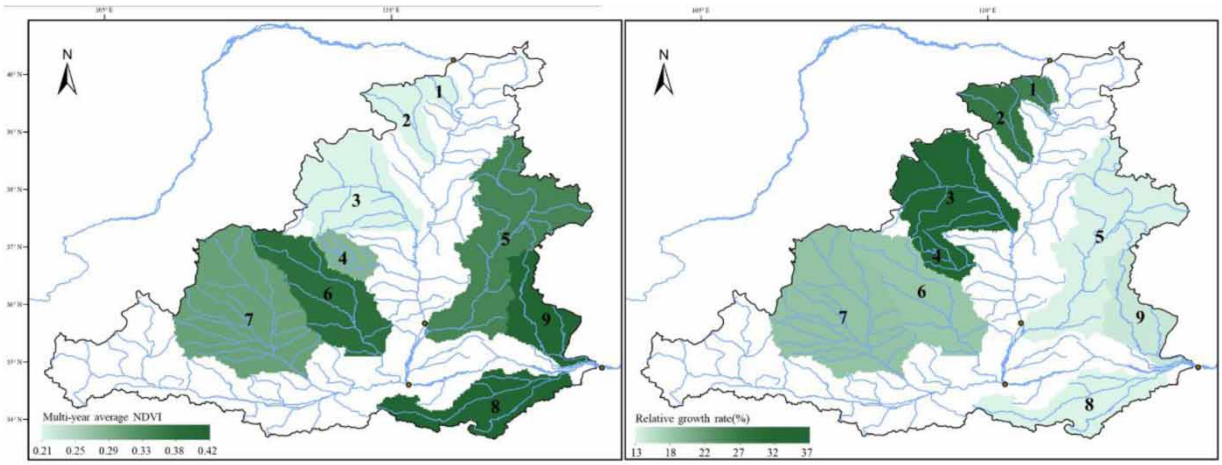

Figure 8 | Spatial distribution of multi-year average NDVI (a) and NDVI growth rate (b) in the study area.

Table 8 | Change of human water use in the MRYR from 1990 to 2020

	Toudaoguai-Longmen		Longmen-Sanmenxia		Sanmenxia-Huayuankou	
	Annual water withdrawal (100 million m^3)	Change rate (%)	Annual water withdrawal (100 million m^3)	Change rate (%)	Annual water withdrawal (100 million m^3)	Change rate (%)
1990–1999	6.3		39.5		21.4	
2000–2009	8.3	31.5	42.3	6.9	16.9	−21.2
2010–2020	12.4	50.6	58.6	38.8	23.1	37.2

Note: Human water withdrawal data are from the Yellow River Water Resources Bulletin for 1990–2020.

Human water withdrawal is also an important reason for the significant decrease in runoff in the MRYR. The Yellow River Water Resources Bulletin shows that human water withdrawal in the MRYR increased from 67×10^8 m^3 in the 1990s to 94×10^8 m^3 in the 2010s (Table 8). Using 1990–1999 as the base period, we calculated the growth rates of human water withdrawals for 2000–2009 and 2010–2020. In both periods, the Toudaoguai-Longmen (Figure 1, including HF, KY, WD, and YR) section experienced significantly higher water withdrawal growth than the other two river sections, according to Table 8.

Spatial differences in human activities lead to significantly higher human activity contributions in HF and KY (with higher NDVI and human water withdrawal growth rates) than in other sub-basins. Therefore, there is a need to develop water resources planning and management plans for sub-basins according to the socio-economic development, land use, and other factors in different sub-basins to cope with future climate change and the impact of human activities on water resources.

4.2. Comparison of results with previous studies

The present study on the contribution of climate and human activities to runoff in nine sub-basins of the MRYR is consistent with the results of previous studies. For sensitivity analysis, the sensitivity of runoff to the underlying surface parameter was shown to be highly dependent on the drought index (E_0/P). The higher the drought index, the greater the sensitivity of runoff to underlying surface change (Berghuijs *et al.* 2017; Li & Quiring 2021). This variation is also evident in our study. Runoff is more sensitive to the underlying surface parameter in the more arid northern sub-basins (Table 5). In addition, both our and previous results show that the sensitivity of runoff to the underlying surface parameter is higher in MRYR than in precipitation and potential evapotranspiration (i.e., $|\phi_n| > |\phi_p| > |\phi_{E_0}|$) (Wang *et al.* 2021; Ni *et al.* 2022). Such a pattern has been verified in other arid basins around the world (Berghuijs *et al.* 2017; Li & Quiring 2021). Li & Quiring (2021) attributed this mainly to the asymmetry of $E_0/P = 1$ in the Budyko equation.

Studies have found that human activities are the main cause of runoff decline in MRYR and its sub-basins, with a contribution rate exceeding 50% (Zhang *et al.* 2008; Hu *et al.* 2020). For the nine sub-basins covered in this study, the contribution of human activities to runoff ranged from 55.1 to 95.8% (Table 6). These findings are generally consistent with the results of previous studies.

However, there are slight differences between our study and earlier work in decomposing the contributions of some sub-basins (Zhao *et al.* 2014; Li *et al.* 2019). For example, in previous studies, human activities contributed between 70 and 85% to reduced runoff in WD (Zhao *et al.* 2014; Li *et al.* 2018). In contrast, our study results were only 58%. It was found that previous studies focused on the period up to approximately 2010. In contrast, based on analysis of watershed hydrometeorological data, precipitation in WD increased sharply in 2011. From 2011 to 2020, the average annual precipitation was 503 mm, which was 25.8% greater than it was before 2011 (Figure 9). Since 2011, there has been a noticeable increase in runoff due to the increased precipitation (Figure 9). Before 2011, the runoff consistently displayed a declining trend. From 2001 to 2010, the runoff was 25.96 mm; after 2011, it was 30.08 mm (2011–2020), suggesting that dominant driving patterns change over time (Li & Quiring 2021).

4.3. Limitations

Some uncertainties and limitations in runoff attribution must be acknowledged. First, there is a strong interaction between vegetation and climate (Liu *et al.* 2006; Strengers *et al.* 2010), making it difficult to fully distinguish between their

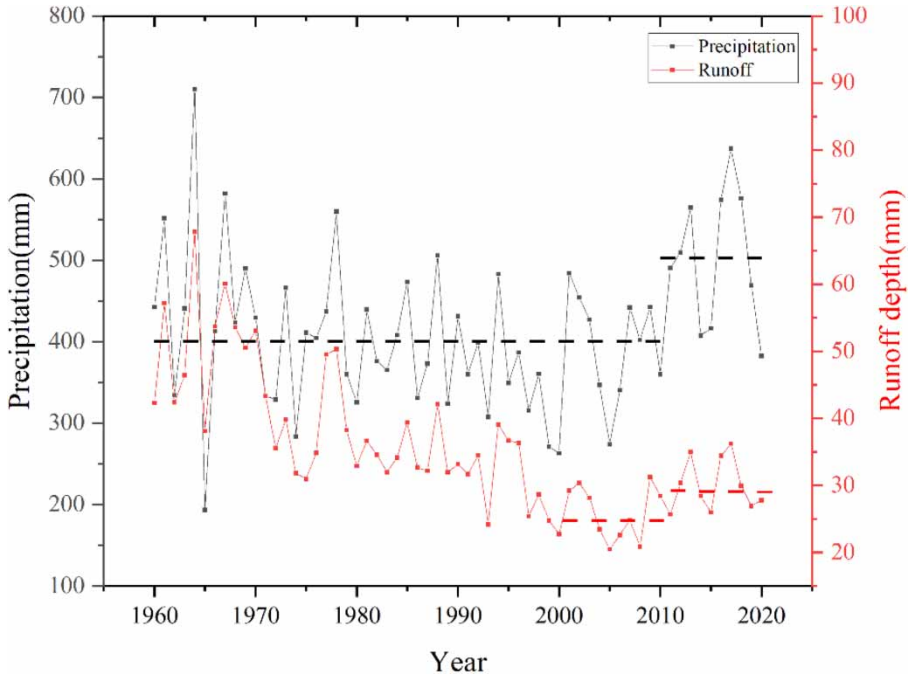

Figure 9 | Trends in precipitation and runoff depth of the WD from 1960 to 2020.

contributions to runoff. In addition, this study did not quantitatively disentangle the contributions of soil and water conservation measures, human water withdrawal, and watershed scale to runoff. This study provides a basis for establishing their quantitative relationships with substrate coefficients and quantitatively calculating the runoff contributions of these human activities.

5. CONCLUSION

This study used the linear propensity estimation method, the M–K test method, and the Budyko hydrothermal coupling balance equation to analyze the variation trends of precipitation, runoff, and potential evapotranspiration in the MRYR and nine typical river basins from 1960 to 2020. The contribution rate of climate change and human activities to the runoff change in the study area is quantitatively decomposed. The main research conclusions are as follows:

(1) MRYR has tended to be drier during the past decades, with decreasing precipitation and increasing potential evapotranspiration. Spatially, the precipitation in the five northern sub-basins (HF, KY, WD, YR, FR) was less than that in the southern region, and the potential evapotranspiration was greater during the 1960–2020 period, indicating a drier condition in the northern sub-basins. A significant decrease in precipitation ($p < 0.01$) could only be detected in QR, while changes in other watersheds were not significant. In addition, the changes of potential evapotranspiration were more different, and the trend of HF, YL, and QH decreased significantly ($p < 0.05$). All other sub-basins increased, with significant trends in WD, FR, and BL ($p < 0.01$). The runoff in MRYR and all sub-basins showed a significant decreasing trend ($p < 0.01$).

(2) We divided the study period into the base period (before the abrupt change point, period I) and change period (after the abrupt change point, period II). Compared with period I, runoff and runoff coefficients decreased in all nine sub-basins during Period II. 2161;. The drought index, underlying surface parameter, runoff sensitivity to rainfall, potential evapotranspiration, and underlying surface parameter increased. Spatially, the sensitivity of runoff to the underlying surface parameter was proportional to the drought index, and the drier the location, the more sensitive runoff was to underlying surface changes. In addition, the sensitivity of runoff to the underlying surface parameter was higher than that of precipitation and potential evapotranspiration. This may be caused by the asymmetry of $E_0/P = 1$ in the Budyko equation.

(3) Using the Budyko hydrothermal coupling balance equation, it was found that compared with the base period, both meteorological changes and human activities in the change period resulted in the reduction of runoff, and human

activities were the main reason for the reduction. Human activities in the HF River and KY River basins contributed more than 90% to the reduction of runoff, and the contribution rate of human activities in other basins was more than 55%. Since the NDVI growth rate and human water withdrawal growth rate are significantly higher in the HF and KY sub-basins, their human activity contributes significantly more than the other sub-basins.

ACKNOWLEDGEMENTS

This study was jointly supported by the National Natural Science Foundation of China (51679252, U2240201) and the National Key Research and Development Program (2017YFC0404401). Acknowledgment for the data support from 'National Earth System Science Data Center, National Science & Technology Infrastructure of China. (http://www.geodata.cn)'. Yanyu Dai acknowledges the China Scholarship Council (CSC) for the scholarship support (No. 202108110149).

DATA AVAILABILITY STATEMENT

All relevant data are included in the paper or its Supplementary Information.

CONFLICT OF INTEREST

The authors declare there is no conflict.

REFERENCES

Barnett, T. P., Adam, J. C. & Lettenmaier, D. P. 2005 Potential impacts of a warming climate on water availability in snow-dominated regions. *Nature* **438**, 303–309. http://dx.doi.org.libproxy1.nus.edu.sg/10.1038/nature04141.

Berghuijs, W. R., Larsen, J. R., Van Emmerik, T. H. & Woods, R. A. 2017 A global assessment of runoff sensitivity to changes in precipitation, potential evaporation, and other factors. *Water Resources Research* **53** (10), 8475–8486. https://doi.org/10.1002/2017WR021593.

Budyko, M. I. 1974 *Climate and Life*. Academic Press, San Diego.

Fu, B. 1981 One the calculation of the evaporation from land surface. *Scientia Atmospherica Sinica* **5** (1), 23–31.

Hou, J. W., Ye, A. Z., You, J. J., Ma, F. & Duan, Q. Y. 2018 An estimate of human and natural contributions to changes in water resources in the upper reaches of the Minjiang River. *Science of the Total Environment* **2018** (635), 901–912. https://doi.org/10.1016/j.scitotenv.2018.04.163.

Hu, C., Zhang, L., Wu, Q., Soomro, S. E. H. & Jian, S. 2020 Response of LUCC on runoff generation process in Middle Yellow River Basin: the Gushanchuan basin. *Water* **12** (5), 1237. https://doi.org/10.3390/w12051237.

Ji, G., Huang, J., Guo, Y. & Yan, D. 2022 Quantitatively calculating the contribution of vegetation variation to runoff in the middle reaches of Yellow River using an adjusted Budyko formula. *Land* **11** (4), 535. https://doi.org/10.3390/land11040535.

Kong, D. X., Miao, C. Y., Wu, J. W. & Duan, Q. Y. 2016 Impact assessment of climate change and human activities on net runoff in the Yellow River Basin from 1951 to 2012. *Ecological Engineering* **91**, 566–573. http://dx.doi.org/10.1016/j.ecoleng.2016.02.023.

Leavesley, G. H. 1994 Modeling the effects of climate change on water resources: a review. *Climatic Change* **28** (1–2), 159–177. https://doi-org.libproxy1.nus.edu.sg/10.1007/BF01094105.

Li, Z. & Quiring, S. M. 2021 Identifying the dominant drivers of hydrological change in the contiguous United States. *Water Resource Research.* **57** (5). https://doi.org/10.1029/2021WR029738.

Li, E. H., Mu, X. M. & Zhao, G. J. 2014 Temporal changes in annual runoff and influential factors in the upper and middle reaches of Yellow River from 1919–2010. *Advances in Water Science* **25** (2), 155–163. (in Chinese)

Li, S., Liang, W., Fu, B., Lv, Y., Fu, S., Wang, S. & Su, H. 2016 Vegetation changes in recent large-scale ecological restoration projects and subsequent impact on water resources in China's Loess Plateau. *Science of the Total Environment* **569**, 1032–1039. https://doi.org/10.1016/j.scitotenv.2016.06.141.

Li, B., Liang, Z., Zhang, J., Wang, G., Zhao, W., Zhang, H. & Hu, Y. 2018 Attribution analysis of runoff decline in a semiarid region of the Loess Plateau, China. *Theoretical and Applied Climatology* **131** (1), 845–855. https://doi.org/10.1007/s00704-016-2016-2.

Li, H. J., Shi, C. X., Zhang, Y. S., Ning, T. T., Sun, P. C., Liu, X. F., Ma, X. Q., Liu, W. & Collins, A. L. 2019 Using the Budyko hypothesis for detecting and attributing changes in runoff to climate and vegetation change in the soft sandstone area of the middle Yellow River basin, China. *Science of the Total Environment* **703**, 13558. https://doi.org/10.1016/j.scitotenv.2019.135588.

Liang, W., Bai, D., Wang, F., Fu, B., Yan, J., Wang, S., Yang, Y., Long, D. & Feng, M. 2015 Quantifying the impacts of climate change and ecological restoration on streamflow changes based on a Budyko hydrological model in China's Loess Plateau. *Water Resources Research* **51**, 6500–6519. https://doi.org/10.1002/2014WR016589.

Liu, Z., Notaro, M., Kutzbach, J. & Liu, N. 2006 Assessing global vegetation–climate feedbacks from observations. *Journal of Climate* **19** (5), 787–814. https://doi.org/10.1175/JCLI3658.1.

Liu, H., Gong, P., Wang, J., Clinton, N., Bai, Y. & Liang, S. 2020 Annual dynamics of global land cover and its long-term changes from 1982 to 2015. *Earth System Science Data* **12**, 1217–1243. https://doi.org/10.5194/essd-12-1217-2020.

Liu, W., Shin, C. X. & Zhou, Y. Y. 2021 Trends and attribution of runoff changes in the upper and middle reaches of the Yellow River in China. *Journal of Hydro-Environment Research* **37**, 57–66. https://doi.org/10.1016/j.jher.2021.05.002.

Luan, J. K., Zhang, Y. Q., Ma, N., Tian, J., Li, X. J. & Liu, D. F. 2021 Evaluating the uncertainty of eight approaches for separating the impacts of climate change and human activities on streamflow. *Journal of Hydrology* **601**. https://doi.org/10.1016/j.JRydrol.2021.126605.

Mann, H. B. 1945 Nonparametric tests against trend. *Econometrica*. https://doi.org/10.2307/1907187.

Miao, C., Ni, J. & Borthwick, A. G. 2010 Recent changes of water discharge and sediment load in the Yellow River basin, China. *Progress in Physical Geography* **34** (4), 541–561. https://doi.org/10.1177/0309133310369434.

Ni, Y. X., Yu, Z. H., Lv, X. Z., Qin, T. L., Yan, D. H., Zhang, Q. F. & Li, M. 2022 Spatial difference analysis of the runoff evolution attribution in the Yellow River Basin. *Journal of Hydrology* **612**, 128149. https://doi.org/10.1016/j.jhydrol.2022.128149.

Piao, S. L., Ciais, P., Huang, Y., Shen, Z. H., Peng, S. S., Li, J. S., Zhou, L. P., Liu, H. Y., Ma, Y. C., Ding, Y. H., Friedlingstein, P., Liu, C. Z., Tan, K., Yu, Y. Q., Zhang, T. Y. & Fang, J. Y. 2010 The impacts of climate change on water resources and agriculture in China. *Nature* **467**, 43–51. http://dx.doi.org.libproxy1.nus.edu.sg/10.1038/nature09364.

Shi, C. X., Zhou, Y. Y., Fan, X. L. & Shao, W. W. 2012 A study on the annual runoff change and its relationship with water and soil conservation practices and climate change in the middle Yellow River basin. *Catena* **100**, 31–41. http://dx.doi.org/10.1016/j.catena.2012.08.007.

Strengers, B. J., Müller, C., Schaeffer, M., Haarsma, R. J., Severijns, C., Gerten, D. & Oostenrijk, R. 2010 Assessing 20th century climate–vegetation feedbacks of land-use change and natural vegetation dynamics in a fully coupled vegetation–climate model. *International Journal of Climatology* **30** (13), 2055–2065. https://doi.org/10.1002/joc.2132.

Sun, G., Zhou, G., Zhang, Z., Wei, X., McNulty, S. G. & Vose, J. M. 2006 Potential water yield reduction due to forestation across China. *Journal of Hydrology* **328** (3–4), 548–558. https://doi.org/10.1016/j.jhydrol.2005.12.013.

Tang, Y. & Wang, Z. G. 2021 Derivation of the relative contributions of the climate change and human activities to mean annual streamflow change. *Journal of Hydrology* **595**. https://doi.org/10.1016/j.JRydrol.2020.125740.

Tian, X., Zhao, G., Mu, X., Zhang, P., Tian, P., Gao, P. & Sun, W. 2019 Hydrologic alteration and possible underlying causes in the Wuding River, China. *Science of the Total Environment* **693**, 133556. https://doi.org/10.1016/j.scitotenv.2019.07.362.

Wang, J. F., Gao, Y. C. & Wang, S. 2018a Assessing the response of runoff to climate change and human activities for a typical basin in the Northern Taihang Mountain, China. *Journal of Earth System Science* **127**, 37. https://doi.org/10.1007/s12040-018-0932-5.

Wang, T., Yang, H., Yang, D., Qin, Y. & Wang, Y. 2018b Quantifying the streamflow response to frozen ground degradation in the source region of the Yellow River within the Budyko framework. *Journal of Hydrology* **558**, 301–313. https://doi.org/10.1016/j.jhydrol.2018.01.050.

Wang, X. B., He, K. N., Li, Y. & Wang, H. 2020 Estimation of the effects of climate change and human activities on runoff in different time scales in the Beichuan River Basin, China. *Human And Ecological Risk Assessment* **26**, 87–103. https://doi.org/10.1080/10807039.2018.1496396.

Wang, Y. B., Wang, S., Wang, C. & Zhao, W. W. 2021 Runoff sensitivity increases with land use/cover change contributing to runoff decline across the middle reaches of the Yellow River basin. *Journal of Hydrology* **600**, 126536. https://doi.org/10.1016/j.jhydrol.2021.126536.

Xing, W., Wang, W., Zou, S. & Deng, C. 2018 Projection of future runoff change using climate elasticity method derived from Budyko framework in major basins across China. *Global and Planetary Change* **162**. https://doi.org/10.1016/j.gloplacha.2018.01.006.

Xu, J. 2011 Variation in annual runoff of the Wudinghe River as influenced by climate change and human activity. *Quaternary International* **244** (2), 230–237. https://doi.org/10.1016/j.quaint.2010.09.014.

Yu, K. X., Zhang, X., Xu, B., Li, P., Zhang, X., Li, Z. & Zhao, Y. 2021 Evaluating the impact of ecological construction measures on water balance in the Loess Plateau region of China within the Budyko framework. *Journal of Hydrology* **601**, 126596. https://doi.org/10.1016/j.jhydrol.2021.126596.

Zhai, R. & Tao, F. L. 2017 Contributions of climate change and human activities to runoff change in seven typical catchments across China. *Science of The Total Environment* **605–606**, 219–229. https://doi.org/10.1016/j.scitotenv.2017.06.210.

Zhang, X., Zhang, L., Zhao, J., Rustomji, P. & Hairsine, P. 2008 Responses of streamflow to changes in climate and land use/cover in the Loess Plateau. *China. Water Resource Research* **44**. https://doi.org/10.1029/2007WR006711.

Zhang, S., Yang, Y., McVicar, T. R. & Yang, D. 2018 An analytical solution for the impact of vegetation changes on hydrological partitioning within the Budyko framework. *Water Resources Research* **54**, 519–537. https://doi.org/10.1002/2017WR022028.

Zhao, G. J., Mu, X. M., Tian, P., Wang, F. & Guo, P. 2013 Climate changes and their impacts on water resources in semiarid regions: a case study of the Wei River basin, China. *Hydrological Processes* **27**, 3852–3863. https://doi.org/10.1002/hyp.9504.

Zhao, G., Tian, P., Mu, X., Jiao, J., Wang, F. & Gao, P. 2014 Quantifying the impact of climate variability and human activities on streamflow in the middle reaches of the Yellow River basin, China. *Journal of Hydrology* **519**, 387–398. https://doi.org/10.1016/j.jhydrol.2014.07.014.

Zhao, Y., Hu, C., Zhang, X., Lv, X., Yin, X. & Wang, Z. 2021 Response of sediment discharge to soil erosion control in the middle reaches of the Yellow River. *Catena* **203**, 105330. https://doi.org/10.1016/j.catena.2021.105330.

Zheng, J., He, Y., Jiang, X., Nie, T. & Lei, Y. 2021 Attribution analysis of runoff variation in Kuye River Basin based on three Budyko methods. *Land* **10** (10), 1061. https://doi.org/10.3390/land10101061.

First received 24 May 2022; accepted in revised form 6 March 2023. Available online 17 March 2023